

Improved Road Crack Detection Utilizing Pixel Categorization with Linear Relationship Based Augmentation in Robust Fuzzy-C Means Clustering

Munish Bhardwaj¹, Nafis Uddin Khan², Vikas Baghel¹

¹Jaypee University of Information Technology, Solan, India

²Department of Artificial Intelligence & Data Science, Faculty of Science and Technology, (IcfaiTech), ICFAI Foundation for Higher Education, Hyderabad, India

E-mail: munish368@gmail.com, nafisuk@ifheindia.org, vikas.baghel@juit.ac.in

Keywords: K-Means clustering, Fuzzy C-Means clustering, road crack detection

Received: March 04, 2025

Roads with many cracks are dangerous, hard to inspect manually and required extensive repairs if left unaddressed. Automating crack detection can save time and money, but it's difficult due to poor image quality. To address this, we present a powerful and novel Fuzzy C-Means clustering method for automating fracture identification. This approach utilizes a 3×3 window that encompasses the whole picture and then categorized the pixels into edge or non-edge pixels using a second order difference equation prior to segmentation. Moreover, it allows for edge pixel augmentation within every window, which effectively highlights the details of fractures. This enhancement employs an augmented scaling factor derived from pixel contribution ratio alongside Michelson contrast to improve the edge and crack detection accuracy. Furthermore, the intensity difference is incorporated to addressing the ambiguity that arises in cluster assignments when Euclidean distances are identical during segmentation, leading to more precise and reliable fracture identification. Additionally, the proposed novel algorithm demonstrates effective crack detection on unfamiliar photographs across various scenarios, without the reliance on a training dataset. The empirical findings indicate that the proposed Fuzzy C-Means Clustering algorithm (called as CLAFCMC) achieves superior performance in term of Partition Entropy, Davies-Bouldin Index, and Partition Index values compared to the existed methods such as K-Means Clustering, Fuzzy C-Means Clustering, and Manhattan distance-based Fuzzy C-Means Clustering for road crack detection. Furthermore, the algorithm optimizes computational efficiency, significantly reducing execution time. These results validate the algorithm's reliability and effectiveness, positioning it as a highly promising solution for automated road crack detection systems.

Povzetek: Obravnava izboljšano metodo zaznavanja razpok na cestnih površinah, ki temelji na kategorizaciji slikovnih točk in razširjanju podatkov z linearnimi relacijami v okviru robustnega fuzzy C-means gručenja. Predlagani pristop izboljša zaznavo razpok v zahtevnih pogojih.

1 Introduction

Road cracks reduce functionality and are often caused by aging infrastructure, rough terrain, and heavy traffic. Consequently, prompt detection is essential to minimize maintenance expenses and ensure safe driving conditions. So, it is crucial to get precise data on road cracks, which can be done manually or automatically [1]. Manual detection methods are laborious and error-prone, whereas automated systems yield faster and more accurate results [2][3][4], though picture noise may compromise their accuracy. Significant work is underway to improve strategies for automated detection algorithms, aiming to enhance their performance in identifying road cracks from photos. The method for detecting cracks in the road image (mention in Figure 1) using a self-collected dataset is based on taking pictures of the areas of the road where cracks are anticipated using a camera or a similar device [2]. The captured photos should be pre-processed to get

rid of extraneous factors that degrade quality. This stage involves converting the photos to grayscale, making subsequent processing faster and more efficient. After pre-processing, the images are segmented to extract specific features. Various methods can differentiate regions with similar pixel characteristics. But clustering, in particular, has proven to be the most effective technique for isolating similar pixels in raw pictures that highlight particular characteristics.

In order to aid in the recognition of road fracture patterns from photographs, the existing clustering approaches such as K-means clustering (KMC) strategy [5][6], the Fuzzy C-Means clustering (FCMC) approach [7][4], Manhattan Distance based Fuzzy C-Means clustering (MHFCM) algorithm [8] are adopted. Further details regarding these are supplied in Section II. Thus, the primary objective of the proposed strategy is to create an innovative and exceptionally effective novel FCM clustering (called as CLAFCMC) approach for fracture autonomous

identification by utilising the knowledge gained from above mentioned existing clustering approaches. Hence, this approach achieves the fracture effectively and also making it feasible to recognise fissures despite low-contrast photographs. To evaluate the proposed algorithm, the variety of road fracture pictures from a personally compiled dataset were utilized. The following are the proposed method's key steps:

- 1) The two-dimensional road images were processed using 3×3 window ($\hat{W}_{dow}^{(3 \times 3)}$), it covers the complete photo.
- 2) The image data were sorted into edge pixels (\hat{E}_{px}^e) and non-edge pixels (\hat{E}_{px}^n) by employing Laplacian-based second-order pixel differentials ($S_{e^{od}}^e$) under image pixel Categorization (\hat{I}_{pix}^{cn}).
- 3) The augmentation of the image's edge pixels (A_{px}^e) has been performed on each $\hat{W}_{dow}^{(3 \times 3)}$ to enhance each \hat{E}_{px}^e .
- 4) Additionally, the intensity difference between maximum and minimum pixels ($i_{max,min}^d(g)$) represents the more precise and reliable fracture identification in an image.
- 5) The experimental findings reveal that the *CLAFCMC* segmentation technique proposed here excels beyond its counterparts—KMC, FCMC, and MHFCM—in accurately identifying a range of road surface anomalies such as alligator, transverse, and longitudinal fractures, along with potholes, within road imagery.

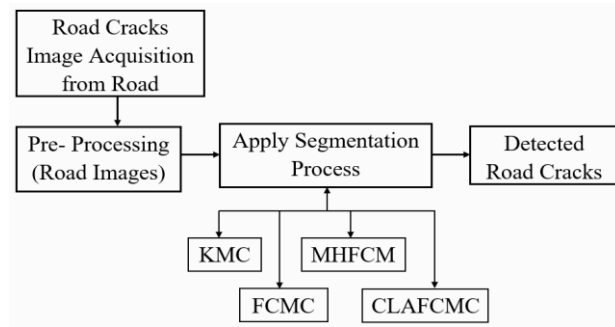


Figure 1: Road cracks detection layout leveraging processing of images

The remaining of paper is structured accordingly: Section II explores a discussion on the KMC and FCMC algorithms, along with their various adaptations. Section III offers comprehensive insights and elucidates the suggested algorithm. Section IV provides the experimental data and discussion, whereas Section V summarizes or conclude our findings and suggests directions for further research.

2 Depiction of fuzzy C-Means clustering algorithms

A concise overview of both traditional & advanced FCMC algorithm, along with the related latest approaches for road cracks recognitions, are presented in this Section.

2.1 Traditional fuzzy C-Means clustering

The renowned FCMC algorithm, which uses an iterative unsupervised learning process [9], was extended by Bezdek et al. [7][4] for photo segmentation. By distributing each data point with a membership degree among several clusters, FCMC works incredibly well in noise-free conditions. The final cluster values are impacted with respect to the closeness to centroids and the strength of membership, maintaining a normalized distribution of memberships [9][10]. The core operations of the traditional FCMC approach are outlined as follows [11][12][13]:

1. The FCMC's Objective function is defined as follows [8]:

$$F_o(\xi, K) = \sum_{a=1}^q \sum_{h=1}^s \xi_{ha}^v \|T_h - K_a\|^2 \quad (1)$$

Where T_h is finite datapoints, K_a is cluster centers, s & q is total pixels & clusters, v is fuzzification parameter & typically, values in the range [1.5-2.5] yield optimal results for image segmentation.

2. At its onset, the membership matrix (ξ_{ha}) is subjected to random initialization through: $\sum_{a=1}^q \xi_{ha} = 1$; where $\xi = [\xi_{ha}]_{q \times s}$ with $0 \leq \xi \leq 1$.
3. Apply the subsequent equation to determine K_a

$$K_a = \frac{\sum_{h=1}^s \xi_{ha}^v T_h}{\sum_{h=1}^s \xi_{ha}^v};$$

$$a=1, 2, 3, \dots, q \text{ and } v > 1 \quad (2)$$

4. Upgrade ξ_{ha} : compute the updated ξ_{hg} using:

$$\xi_{ha} = \frac{\left[\frac{1}{D_{ha}} \right]^{\frac{1}{v-1}}}{\sum_{c=1}^q \left[\frac{1}{D_{hc}} \right]^{\frac{1}{v-1}}} \quad (3)$$

Where $D_{ha} (= \|T_h - K_a\|)$ is Euclidean distance

5. The iterative procedure concludes when the $\|\xi^{(L+1)} - \xi^{(L)}\|$ falls below the positive threshold, designated as δ . In this context, L signifies the iteration index. Or either return to stage number 3 and continue the process till fixed number of centroids achieved.

FCMC approach work well in segmenting noise-free images but face challenges with images containing noise and artifacts. This is mainly due to their inability to account for neighboring pixel interactions, making computational time management less efficient [9][14].

2.2 Advanced Fuzzy C-Means clustering

Road crack detection by hand is time-consuming and prone to errors, which emphasises the requirement of an approach that can reliably identify fractures from new photographs under a variety of environmental conditions. The FCMC is gaining recognition as an effective unsupervised clustering technique for image

segmentation and has been successfully used to detect fractures, but its application to automated road crack detection is limited. Consequently, the advanced FCMC algorithms employed in road crack detection are given below:

Noh et al. [15] showcased an approach for identifying rifts in concrete images, employing FCMC & various noise mitigation strategies for segmentation. Nonetheless, success rate of crack reorganization significantly declines in clusters with significant noise that contain fractures. Bhard et al. [3] present an algorithm for automatic fracture detection, incorporating optimal enhanced edge pixels and fuzzy factors. By analyzing the intensities of both edge & non-edge pixels, the technique accurately detects edges in low-contrast pictures without necessity of training datasets or complicated parameter tuning. Consequently, this leads to enhances fracture detection and outperforms existing techniques.

To lessen noise from the background and improve image smoothness, Oumaa et al. [17] use a multi-scale wavelet transform filtering technique. Later, they apply a better method of pothole detection and classification by using morphological refinement and unsupervised FCM clustering. Their strategy also demonstrates accuracy in estimating the shapes and sizes of potholes. In order to integrate Manhattan distance (M_{dis}) and histogram equalization (h_{eaz}) inside the FCMC framework, Bhardwaj et al. [8] utilize the MHFCM approach. The integration of M_{dis} enhances accuracy by measuring dissimilarity between the dataset and cluster centroids, thereby improving cluster distinction. Furthermore, total picture contrast is improved by h_{eaz} . Therefore, the MHFCM method proves effective in identifying distinct kind of road cracks in photo. The mathematical illustration of the M_{dis} & h_{eaz} is given below:

$$(M_{dis})_{ha} = |T_h - K_a| \quad (4)$$

Whereas $a = 1, 2, 3, \dots, q$ and $h = 1, 2, 3, \dots, s$

$$h_{eaz}(o) = P(x_o) = \frac{T_o}{s}; 0 \leq o \leq a-1 \quad (5)$$

Whereas a & s represent the total number of gray levels & pixels, respectively, T_o denotes the total count of pixels corresponding to identical intensity level o . Although the MHFCM is effective in fracture detection but it has a number of drawbacks. The h_{eaz} process affects the entire image by enhancing overall contrast, but it may sacrifice the local details near boundaries and edges. Furthermore, for best results, both h_{eaz} and FCMC require proper parameterization, which introduces processing difficulties into the MHFCM architecture. Combining these methods can further increase complexity and lead to longer processing times, particularly for large-scale images.

2.3 Literature survey

Innovating approaches for the quick identification of road cracks are shown by Cubero et al. [16], who also show how to use these techniques to extract key

characteristics required for the cracks' identification. In the end, a decision tree heuristic approach is used to classify an image. According to Bhard et al. [6], KMC requires a preset amount of clusters, which can be difficult to accomplish when working with complex or high-dimensional data. Shi et al.'s automated system [18] lowers noise while diagnosing road rifts by understanding the fundamental structural properties of cracks. Wang et al. [19] claim that pavement picture virtue is essential for fracture identification. However, shadows and shadow-like noises are often present in these images. These can come from telegraph poles, buildings, trees, lights, lamps, and other items. To get over this problem and extract pavement fractures from a shaded photograph, an image processing technique is proposed.

The author et al. [20] introduce an innovative crack detection method for road maintenance, overcoming the limitations of current techniques. The approach, built upon Faster-RCNN, incorporates an optimized feature extraction network, leading to better accuracy and generalization across diverse conditions. Real-world testing demonstrates its potential to replace time-consuming traditional methods, offering a practical and efficient solution for road crack detection.

A novel method for identifying pavement cracks is presented by Xiaoran et al. [21], which use a deep convolutional neural network fusion model. It integrates the benefits of both the U-Net model and the SSD convolutional neural network. To increase identification confidence, the model is first applied to categorize and identify cracks. The pavement cracks are then precisely defined using a fracture segmentation network. The precession of classifying and segmenting pavement fractures has significantly improved due to advancements in feature extraction structure and model hyper parameter optimization. Ultimately, the segmentation findings are used to determine the length, breadth (for linear fractures), and area (for alligator rifts). Firstly, to enhance the suppression of noise and edge feature extraction, the authors Jie et al. [22] integrate the bilateral filter and the four-way Sobel operator into the Canny method. Following non-maximum repression, gradient information is adaptively used to establish a dynamic threshold. Following morphological analysis of the detection map and region-wise grading, the bilateral filter variables are adjusted according to the results of recognition. The convolutional feature extraction module is subsequently utilized to create the Canny Road crack detection map. It first fuses the lower feature layer of the DeepLab V3+ detection network together its higher feature layer. The final map is produced using convolutional feature extraction.

This paper presents the novel pixel-level semantic segmentation network, known as Crack W-Net, as introduced by Chengjia et al. [23]. Convolutional neural networks with a skip-level round-trip sampling block structure are employed to develop it. A method for identifying road fractures based on deep learning principles is described by Li et al. [24]. It suggests a novel activation function called MeLU, an innovative differentiable computing method, and an original

architecture called DDLCN (Deep Dictionary Learning and Encoding Network). The standard Mask-RCNN algorithm, which was enhanced by specific enhancements, serves as the foundation for this technique. Evaluation juxtapositions demonstrate significant benefits in terms of F1-score, recall, and accuracy.

By combining an attention mechanism with multiscale dilated convolutions to improve extraction of features, Weidong et al. [25] present an efficient fracture detecting network. To achieve precise identification, a module for up sampling integrates layer attributes. Severity of fractures is determined by assessing the width and fork division, and they can be categorized as transversal, longitudinal, block, or alligator forms. The authors of the work, Jong et al. [26], successfully handle the challenge of gathering datasets by employing a data augmentation technique focused on learning about fracture thickness and detection. This is a money- and time-efficient process. Moreover, a method of adaptively processing fracture data is introduced to improve efficiency. The method entails building a quad tree depending on the occurrence of cracks. The crack detection technology is tested in a variety of scenarios in order to confirm the degree of precision gain. According to IoU (Intersection over Union), the outcomes demonstrate superior precision in every scenario. The false detection rate is about 25% when the system operates in the absence of extra crack data. But with the augmentation mechanism in place, the rate of false positives is significantly reduced. The authors et al. [30] propose a hybrid crack detection method combining noise-tolerance and edge precision, outperforming CrackIT and deep learning methods (HED, RCF, FPHB) on standard datasets while reducing discretization errors.

The author et al. [31] proposes leveraging explainable AI (XAI) to generate segmentation masks with weak supervision, reducing labeling efforts. While less precise than supervised methods, the approach effectively supports crack severity and growth monitoring. The author et al. [32] use Fast Point Feature Histograms (FPFH) and a specially designed 3D PatchCore algorithm to suggest a way to use point clouds and geometric distortions to find cracks in masonry arch bridges. Experiments on artificial point clouds created using 3D FEM demonstrate that the approach is reliable contrary noise, damage, & surface roughness while detecting both internal and external cracks. However, it still has difficulties in identifying small curvature and in-plane distortions.

Therefore, to address the shortcomings of current methods, an effective technique for pixel classification and pixel enhancement is essential, utilizing a 3×3 window. The classification approach distinguishes edge and non-edge pixels. Then after, a scaling factor is applied to enhance edge pixels before segmentation, improving pixel detail and contrast. Incorporating all in the segmentation process strengthens extracting features, suppresses noise, optimizes clustering, & sharpens borderline accuracy. These innovative capabilities are

integrated into the suggested approach, as explained in Section 3.

3 Proposed method

In this Section, we describe an innovative and beneficial approach to diagnosing road fractures. We have introduced a proficient or novel method for recognizing fractures, leveraging Fuzzy C-Means Clustering, known as the *CLAFCMC* methodology, specifically designed for detecting road cracks. This novel approach incorporates the image pixel Categorization (\hat{I}_{pix}^{cn}) and augmentation of the image's edge pixels (A_{px}^e). The aim of this strategy is to tackle the shortcomings and problems associated with the techniques discussed in Section II. Consequently, this technique utilizes a 3×3 window ($\hat{W}_{dow}^{(3 \times 3)}$) (as depicted in Fig. 2) that spans the entire image $K \times l$ to implement the \hat{I}_{pix}^{cn} . The A_{px}^e is essential for highlighting more intricate details and improving feature discernment while preparing picture data for assessment. Therefore, prior to segmentation, pixels undergo the enhancement using augmented scaling factor with in $\hat{W}_{dow}^{(3 \times 3)}$ for reliable fracture detection. Additionally, the intensity difference between maximum and minimum pixels ($i_{max,min}^d(g)$) utilized in segmentation, ensuring precise and reliable fracture detection. Consequently, this proposed algorithm intensifies the contrast between discrete areas or objects in photo, improving clustering as well as boundary definition & culminating in better results. The details of \hat{I}_{pix}^{cn} and A_{px}^e for *CLAFCMC* approach is elaborated upon below:

3.1 Image pixel categorization in 3×3 window

The \hat{I}_{pix}^{cn} , categorises the image pixels inside a $\hat{W}_{dow}^{(3 \times 3)}$ using a S_e^{od} , shown in Fig. 2. This categorization efficiently distinguishes into edge pixels (\hat{E}_{px}^e) & non-edge pixels (\hat{E}_{px}^n) before the segmentation procedure.

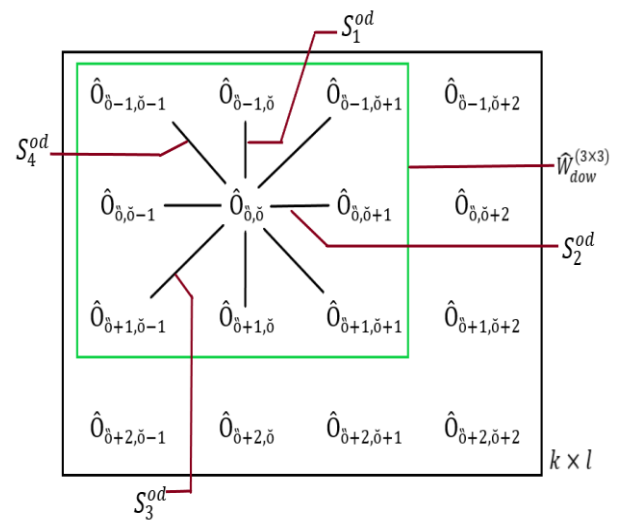


Figure 2: S_e^{od} of the central pixel in $\hat{W}_{dow}^{(3 \times 3)}$ purlieus in four directions

Thus, the mathematical expression corresponding to the $\hat{W}_{dow}^{(3 \times 3)}$ tactic can be articulated as follows [27]:

$$\hat{W}_{dow}^{(3 \times 3)} = [\hat{O}_{\delta+\tilde{l}, \delta+\tilde{t}}] \quad (6)$$

for $\tilde{l} = t \text{ to } t + 2$ and $\tilde{t} = q \text{ to } q + 2$

for $t = -1, 0, 1, 2, \dots, k - 2$ and $q = -1, 0, 1, 2, \dots, l - 2$

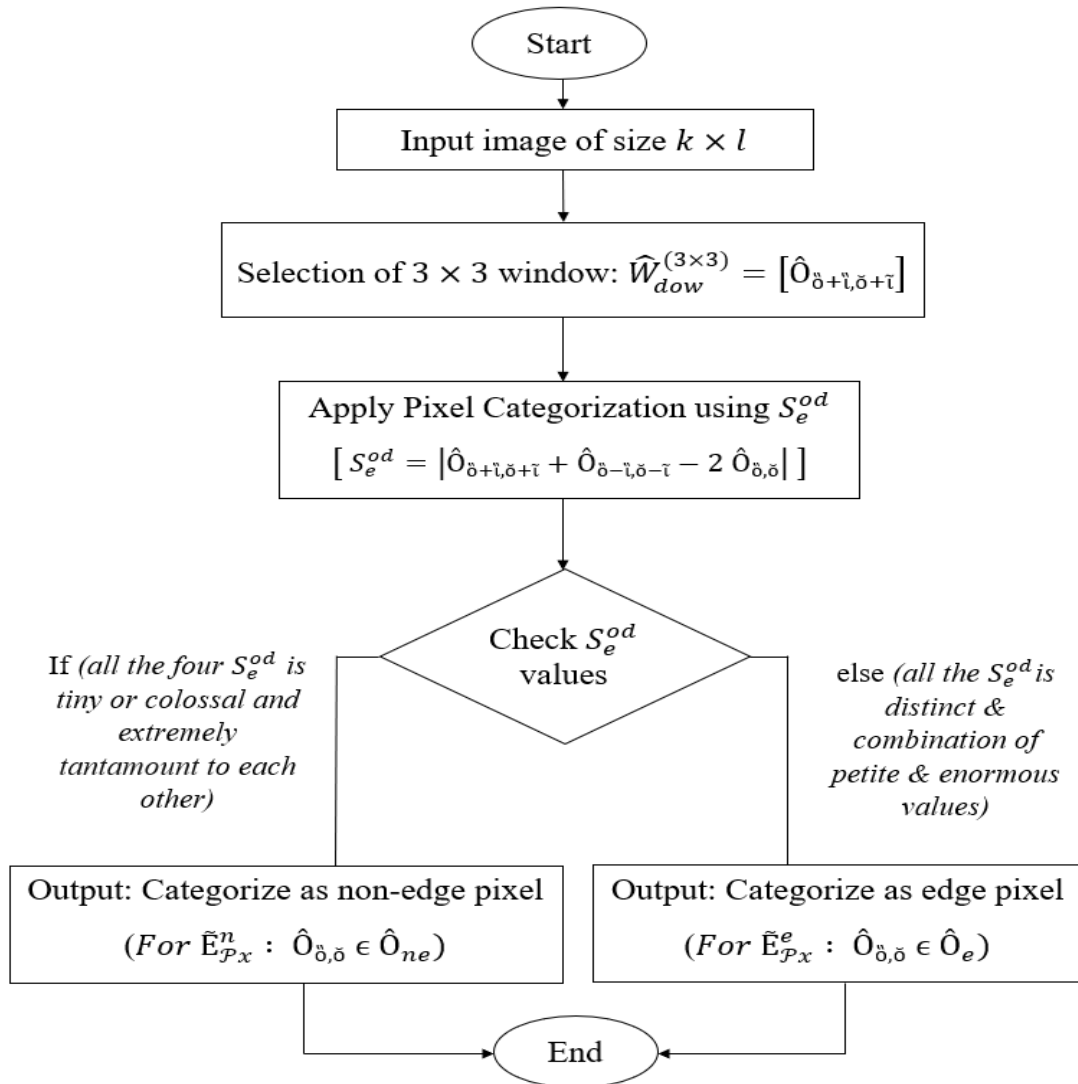


Figure 3: The flowchart of image pixel categorization in 3×3 window

Whereas $\hat{O}_{\delta+\tilde{l}, \delta+\tilde{t}}$ signifies the individual pixels within $\hat{W}_{dow}^{(3 \times 3)}$, \tilde{l} and \tilde{t} indicate the row and column in the same window, δ & δ determine the outset indices or offsets (i.e., δ , δ is equal to one and so on) and k , l is total count of rows and columns of photograph. Specifically, the rows down from δ represented by \tilde{l} , while the columns to the right of δ are represented by \tilde{t} . Implemented together, δ & δ , \tilde{l} & \tilde{t} pinpoint an element's exact location inside the frame ($\hat{W}_{dow}^{(3 \times 3)}$). The middle pixel of $\hat{W}_{dow}^{(3 \times 3)}$ is utilised to compute S_e^{od} [27] in four aloof directions (lateral, longitudinal, oblique, and contrary oblique), as specified in Eq. (7).

$$S_e^{od} = |\hat{O}_{\delta+\tilde{l}, \delta+\tilde{t}} + \hat{O}_{\delta-\tilde{l}, \delta-\tilde{t}} - 2 \hat{O}_{\delta, \delta}| \quad (7)$$

Where the values supplied for $(e, \tilde{l}, \tilde{t})$ parameter set is [(1, 0, 1), (2, 1, 0), (3, -1, 1), and (4, 1, 1)], represents the four

flanks. In order to differentiate between the two-pixel classes as outlined in flowchart in Figure 3, it is necessary to analyses the S_e^{od} in all four directions relative to each examined pixel. Therefore, this S_e^{od} is able to evaluate the entire pixels of photo.

3.2 Augmentation of the image's edge pixels utilizing 3×3 window

The augmentation of the image's edge pixels ($A_{\mathcal{P}_x}^e$) is employed to diligently refine each edge pixel ($\tilde{E}_{\mathcal{P}_x}^e$) in $\hat{W}_{dow}^{(3 \times 3)}$ of $k \times l$ image after \hat{I}_{pix}^{cn} to obtain higher-quality edge regions. Therefore, it is imperative to pay great attention to determining the augmented scaling factor (\hat{A}_{SF}^{um}) is crucial for effective enhancement of the original $\tilde{E}_{\mathcal{P}_x}^e$ value. This \hat{A}_{SF}^{um} can be computed using an equation that resembled with (or based-on) linear equation called as

linear relationship based equation. Hence, anomalies may arise in the image, if \tilde{A}_{SF}^{um} for \tilde{E}_{px}^e is set too high, causing exaggerated edges, resulting in an unnatural appearance. Conversely, very tiny values may result in a loss of clarity and sharpness, which may dull or washes out the image. Consequently, using the best approach is necessary to preserve edge quality. Thus, the following is the mathematical expression for augmented edge pixels (\tilde{O}_e), which is obtained by examining both the $[\hat{O}_e]$ and \tilde{A}_{SF}^{um} :

$$[\tilde{O}_e] = [\tilde{A}_{SF}^{um}]_e \times [\hat{O}_e]; \quad \text{for } e = 1, 2, 3, \dots, \check{a} \quad (8)$$

Whereas \check{a} is the entire number of edge pixels in $\hat{W}_{dow}^{(3 \times 3)}$ and \hat{O}_e is the unique edge pixel value in $\hat{W}_{dow}^{(3 \times 3)}$ found after \hat{f}_{pix}^{Cn} . The \tilde{A}_{SF}^{um} in a $\hat{W}_{dow}^{(3 \times 3)}$ is attained by employing the edge pixel contribution ratio (\check{C}_e^{pxr}) and constant ratio (\check{C}_{const}), as articulated by the following mathematical expression:

$$[\tilde{A}_{SF}^{um}]_e = 1 + \check{C}_e^{pxr} \times \check{C}_{const} \quad (9)$$

Whereas the $\check{C}_e^{pxr} (= \hat{O}_e / \sum_{v=1}^a \hat{O}_v)$ is the ratio of each individual \tilde{E}_{px}^e to total \tilde{E}_{px}^e with in $\hat{W}_{dow}^{(3 \times 3)}$ and the \check{C}_{const} is the ratio of the difference among the maximum & minimum of the \tilde{E}_{px}^e value to their sum (based on Michelson contrast). Hence the $\check{C}_e^{pxr}, \check{C}_{const}$ allows to acquiring the local information in term of weight of nearby individual \tilde{E}_{px}^e within the $\hat{W}_{dow}^{(3 \times 3)}$. The Eq. (9) furnishes the \tilde{A}_{SF}^{um} , which, when applied, enables the augmentation of the edge pixel. Therefore, this processed image is then input into the segmentation process (mentioned in sub-section 3.3) for precise crack detection, ensuring accuracy despite noise and lighting variations. The algorithm 1 carries out this augmentation process.

Algorithm 1: Augmentation of the edge pixels

1. Input: $k \times l$ size photo, \hat{O}_e after \hat{f}_{pix}^{Cn}
2. Initialization Parameters:
 - Window size: 3×3
 - The representation of the row and column: \check{l} and \check{t} .
3. Procedure:
 - Iteration begins
 - a. Apply $\hat{W}_{dow}^{(3 \times 3)}$ %% Using the Eq. (6)
 - b. Outer Loop ($e = 1: \check{a}$): Iterate until the last \tilde{E}_{px}^e in $\hat{W}_{dow}^{(3 \times 3)}$ is reached.
 - c. Inner Loop ($v = 1: a$): Iterate until the $\hat{W}_{dow}^{(3 \times 3)}$'s \tilde{E}_{px}^e accumulation is achieved.
 - d. Compute: \check{C}_e^{pxr} & \check{C}_{const}
 - e. Compute the augmented edge Scaling factor:

$$[\tilde{A}_{SF}^{um}]_e = 1 + \check{C}_e^{pxr} \times \check{C}_{const}$$

%% Using Eq. (9)
 - f. Find Augmented Pixels:

$$[\tilde{O}_e] = [\tilde{A}_{SF}^{um}]_e \times [\hat{O}_e] \quad \text{%% Using eqn. (8)}$$

- Iterations Stop Conditions:
 - a. Terminate inner loop: when v reaches a within $\hat{W}_{dow}^{(3 \times 3)}$.
 - b. Terminate outer loop: when e reaches \check{a} with in $\hat{W}_{dow}^{(3 \times 3)}$.
 - 4. Proceed to the subsequent iterations: Iterate until all \tilde{E}_{px}^e of image $k \times l$ are augmented.
 - 5. Output: The outcome depicts the augmented pixels $[\tilde{O}_e]$ for whole picture $k \times l$. Ahead such augmented pixels are employed in the segmentation procedure.
-

As outlined above, the 3×3 window is essential and utilized in pixel categorization and edge pixel augmentation. As this window moves across the image, it helps in differentiates edge and non-edge pixels while enhancing edge pixel details and crack visibility. Additionally, the smaller windows (2×2) lack contextual depth, making clustering noise-sensitive, while larger ones ($4 \times 4, 5 \times 5$) over-smooth the image, blurring critical boundaries. The 3×3 window provides the optimal balance, reducing noise while preserving fine details, ensuring precise segmentation and efficient computation.

3.3 Exhaustive explication of the CLAFCMC

The precise detection of road fractures is the aim of the sturdy and efficient CLAFCMC technology. Hence the objective function of CLAFCMC technique is as described below:

$$\mathcal{U}(\phi, Y) = \sum_{h=1}^c \sum_{g=1}^r \phi_{hg}^p \times \|\hat{O}_g - Y_h\|^2 \times i_{max.,min.}^d(g) \quad (10)$$

where c & r describes the number of clusters & number of pixels in picture, \hat{O}_g is finite input data (under \hat{O}_g : \tilde{O}_e & \hat{O}_{ne} exist), the cluster center is denoted by Y_h , the fuzzy membership matrix is represented by ϕ_{hg} ($0 \leq \phi_{hg} \leq 1$) with $h = 1, 2, 3, \dots, c$ and $g = 1, 2, 3, \dots, r$, p is fuzzification parameter ($p > 1$), controlling the degree of fuzziness in clustering. For optimal image segmentation, p typically falls within the 1.5 to 2.5 range, maintaining a balance among precision and computational effectiveness and the $i_{max.,min.}^d(g)$ indicates the intensity difference among maximum and minimum pixels in $k \times l$ picture. Leveraging $i_{max.,min.}^d(g)$ aids in addressing the ambiguity that arises in cluster assignments when Euclidean distances are identical. Consequently, it leads to a more accurate and refined membership matrix.

To mitigate the function $\mathcal{U}(\phi, Y)$, $\mathcal{U}(\phi, Y)$ Lagrange multiplier method is employed. As indicated below, this

method establishes the updated membership degrees and cluster centres in *CLAFCMC*:

$$L_{multiplier} = \sum_{h=1}^c \sum_{g=1}^r \phi_{hg}^p \times \|\hat{O}_g - Y_h\|^2 \times i_{max,min}^d(g) + \sum_{g=1}^r \delta \left(1 - \sum_{h=1}^c \phi_{hg} \right) \quad (11)$$

To ascertain the membership function, first apply the partial derivative of $L_{multiplier}$ with regards to ϕ_{gh}^p and setting it to zero. Additionally, adopt the derivative of $L_{multiplier}$ with regards to the δ ($\frac{\partial L_{multiplier}}{\partial \delta} = 0$). Therefore, the resulting membership function is given by:

$$\phi_{hg} = \frac{\left[\frac{1}{d_{hg}} \right]^{\frac{1}{p-1}}}{\sum_{g=1}^c \left[\frac{1}{d_{fg}} \right]^{\frac{1}{p-1}}} \quad (12)$$

Whereas δ is Lagrange multipliers. In a similar vein, acquiring cluster centroid involves calculating the partial derivative of $L_{multiplier}$ relative to Y_h , represented as $\frac{\partial L_{multiplier}}{\partial Y_h} = 0$. Once this is derived, the centroid is eventually obtained as follows:

$$Y_h = \frac{\sum_{g=1}^r \phi_{hg}^p \times \hat{O}_g \times i_{max,min}^d(g)}{\sum_{g=1}^r \phi_{hg}^p} \quad (13)$$

The subsequent details elucidate the process of the *CLAFCMC* algorithm as delineated in algorithm 2:

Algorithm 2: CLAFCMC algorithm

1. Input: $k \times l$ size road photo
2. Initialization Parameters:
 c is count of clusters, \hat{O}_g indicates augmented pixels of photo, r is total count of pixels of photo, Y_h is cluster center, p is fuzzification parameter, ϕ_{hg} the fuzzy membership matrix
3. Procedure:
 - a. Outer Loop (h): Encore for every value in c
 - b. Inner Loop (g): Encore for every value in r
 - c. Randomly initialization: $\phi_{hg} = 1$
 $\% \phi = [\phi_{hg}]_{c \times r}$ with $0 \leq \phi_{hg} \leq 1$
 - d. Terminate inner loop: when g reaches r
 - e. Terminate outer loop: when h reaches c
 - f. Initialize: $\eta = 0$ $\% \%$ Iteration index (η)
 - g. Outer Loop (h): Encore for every value in c
 - h. Inner Loop (g): Encore for every value in r
 - i. Compute Y_h : $Y_h = \frac{\sum_{g=1}^r \phi_{hg}^p \times \hat{O}_g \times i_{max,min}^d(g)}{\sum_{g=1}^r \phi_{hg}^p}$
 - j. Compute & update new ϕ_{hg} :

$$\phi_{hg} = \frac{\left[\frac{1}{d_{hg}} \right]^{\frac{1}{p-1}}}{\sum_{g=1}^c \left[\frac{1}{d_{fg}} \right]^{\frac{1}{p-1}}} \% d_{hg} = \|\hat{O}_g - Y_h\|$$

- k. Terminate inner loop: when g reaches r
 - l. Terminate outer loop: when h reaches c
 - m. Until tantamount Y_h emerges, increment $\eta = \eta + 1$ or go back to step f.
 4. Output: Road cracks identification in $k \times l$ size photo
-

In contrast to traditional FCMC, which relies on Euclidean distance and often misclassifies pixels. The proposed method enhances road crack detection by efficiently detecting cracks and minimizing noise and outliers. This leads to an improved distinction between crack and non-crack regions, resulting in more precise segmentation. The novel *CLAFCMC* enhances crack visibility through pixel classification and edge pixels augmentation while integrating intensity difference to refine the visibility of cracks. This ensures precise crack detection, even under challenging conditions like uneven lighting and surface irregularities.

4 Analysis and outcomes of the experimental

This part examines & juxtaposition the findings of the *CLAFCMC* algorithm with several other strategies, including KMC, FCMC, and MHFCM, all implemented in MATLAB. The evaluation occurred on PC with an Intel Core i7 processor at 1.80 GHz, Eight GB of RAM, & running on 11 Microsoft Windows. The parameters c and p seemed both specified as two enabling the algorithms to execute. It ensuring clear distinction between cracks and surrounding regions. This allows segmentation into two clusters—crack and non-crack areas—maintaining uniform conditions across all fuzzy algorithm variations in our simulations. Several types of rifts & flaws, such as transverse (Tv_{crk}), longitudinal (Ln_{crk}), alligator cracks (Ar_{crk}) & pathole (Pa_h), are depicted in this simulation from various road pictures. The Ln_{crk} emerges longitudinally across the road due to poor joints & fatigue from traffic [16]. A Tv_{crk} emerges perpendicular to the road's center line and caused by thermal contraction due to temperature changes. Lackcluster strength in the asphalt substrate is the main ingredient of Ar_{crk} appearance. Pa_h is a significant structural deterioration that occurs whenever precipitation seeps through the earth beneath the surface of the road and expands and shrinks [17].

For road crack detection, input images are selected from a self-acquired dataset to ensure robustness across various crack types, lighting conditions, and noise levels. The dataset was captured using a Samsung camera with 64-megapixel on National Highway (NH)-154 in Himachal Pradesh, India. The images taken during daylight hours under diverse environmental conditions, including sunny, dry, and wet surfaces. This dataset is

employed to assess the effectiveness of the suggested technique during testing.

Despite the availability of the high-resolution imaging, cracks detection remains challenging due to several image quality limitations. The variations in camera perspective (angle and distance) along with motion blur can reduce image clarity and hinder accurate cracks recognition. Additionally, lighting inconsistencies such as glare, shadows, and low light may distort or obscure cracks visibility. The surface noise and environmental factors like contamination, dirt, dust, rain, fog introduce artifacts that effectively hide cracks, making them difficult to detect. These factors highlight that the effective crack detection depends not only on high image resolution but also on the effectiveness and ability of the detection algorithm.

Therefore, the juxtaposition has been performed among the suggested method and previous approaches, namely KMC [5][6], FCMC [7][4], and MHFCM [8]. With self-collected datasets comprising both defiled and non-defiled road images, it outperforms in terms of Partition Entropy (P_{ent}) [28][29], the Davies-Bouldin Index (D_{BI}) [28][29], the Partition Index (P_{ind}) [28][29], and overall execution time ($E_{x\ time}$).

However, like any other method, the *CLAFCMC* may have challenges in the situation of detecting extremely high faint cracks or when extremely low-quality images affected by noise, or low resolution. The empirical findings for the already mentioned picture disciplines are described in Sections 4.1 and 4.2.

4.1 Non-Paint-Water strap on the images of road

The investigation compares the metrics for KMC, FCMC, MHFCM, and *CLAFCMC* for the several visual representations displayed in Fig. 4. Compared to MHFCM, both KMC and FCMC produce poorer outcomes in road fracture identification (Fig. 4: (b-d)). Despite this, MHFCM tends to exhibit fewer disturbances but faces challenges in accurately detecting fractures (Fig. 4: (d)). On the aspects of noise and reliability, the *CLAFCMC* method (Fig. 4: (e)) significantly outperforms the other techniques, delivering superior and more valuable results. Moreover, *CLAFCMC* excels in differentiating between cracked and non-cracked pixels with greater ease than the other methods.

In order to quantitatively access the performance of various techniques for various fracture pictures, we employed P_{ent} , D_{BI} , P_{ind} , and $E_{x\ time}$. Accurate identification and evaluation depend on more effective clustering, which is represented by the lower values of P_{ent} , D_{BI} and P_{ind} . The values of P_{ent} , D_{BI} , P_{ind} and $E_{x\ time}$ represent in Table 1.

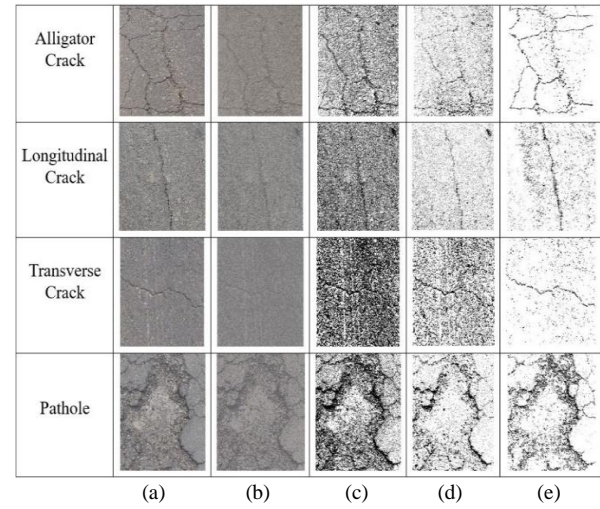


Figure 4: Crack detection: (a) Original image, (b) KMC, (c) FCMC, (d) MHFCM, (e) *CLAFCMC*

Table 1: Comparative analysis of Crack Detection Performance among KMC, FCMC, MHFCM & *CLAFCMC* for Non-Paint-Water- Strap Images

Type of cracks	Parameters	KMC	FCMC	MHFCM	<i>CLAFCMC</i>
Ar_{crk}	P_{ent}	0.15	0.22	0.13
	D_{BI}	0.62	1.08	0.97	0.61
	P_{ind}	0.23	0.20	0.09
	$E_{x\ time}$	4.83	12.74	17.62	10.16
Ln_{crk}	P_{ent}	0.13	0.20	0.11
	D_{BI}	0.54	0.90	0.94	0.50
	P_{ind}	0.17	0.19	0.07
	$E_{x\ time}$	6.51	16.65	20.83	14.34
Tv_{crk}	P_{ent}	0.16	0.24	0.15
	D_{BI}	0.69	1.16	1.02	0.67
	P_{ind}	0.31	0.26	0.14
	$E_{x\ time}$	4.42	13.59	18.43	9.71
Pa_h	P_{ent}	0.14	0.21	0.12
	D_{BI}	0.61	1.02	0.96	0.59
	P_{ind}	0.22	0.21	0.11
	$E_{x\ time}$	4.71	13.48	18.21	10.20

Therefore, the *CLAFCMC* provides valuable insight on fracture recognition since it performs better than others approach in terms of P_{ent} , D_{BI} , P_{ind} and $E_{x\ time}$ for all types of fractures.

The KMC technique has an effective D_{BI} and a shorter $E_{x\ time}$ when compared to other approaches. Nonetheless, the simulation findings indicate that it performs less well than *CLAFCMC* in terms of D_{BI} . Therefore, it is evident from the thorough data shown in Table I and Figure 4 that *CLAFCMC* performs better than others.

4.2 Paint-Water strap on the images of road

This Section discusses the several types of flaws that can be seen in road pictures, like paint and water. The results involve a comparative analysis of different

algorithms across various images, as shown in Fig. 5 (a). The data reveal that MHFCM surpasses KMC & FCMC approaches in certain aspects of effectiveness, as illustrated in Fig. 5 (b–d). When compared to *CLAFCMC*, MHFCM has a number of serious flaws, such as noise, paint and water traces, and blurring, as seen in Fig. 5 (d–e). The *CLAFCMC* method outperforms similar algorithms in terms of noise reduction, execution time, and effectively identifying boundaries in the surrounding area.

Table 2: Comparative analysis of crack detection performance among KMC, FCMC, MHFCM & *CLAFCMC* for paint-water strap images

Types of Cracks	Parameters	KMC	FCMC	MHFCM	<i>CLAFCMC</i>
Ar_{crk}	P_{ent}	0.17	0.25	0.14
	D_{Bl}	0.65	1.34	0.97	0.62
	P_{ind}	0.27	0.25	0.12
	$E_{x\ time}$	5.02	13.27	18.23	10.12
Ln_{crk}	P_{ent}	0.13	0.21	0.11
	D_{Bl}	0.58	0.98	0.94	0.57
	P_{ind}	0.19	0.20	0.10
	$E_{x\ time}$	6.97	18.45	20.91	16.07
Tv_{crk}	P_{ent}	0.12	0.18	0.09
	D_{Bl}	0.55	0.96	0.92	0.52
	P_{ind}	0.18	0.17	0.06
	$E_{x\ time}$	5.71	25.74	20.15	18.17
P_{ah}	P_{ent}	0.15	0.22	0.13
	D_{Bl}	0.61	1.01	0.95	0.60
	P_{ind}	0.23	0.21	0.08
	$E_{x\ time}$	9.58	46.25	35.06	32.08

The current model determining the P_{ent} , D_{Bl} , P_{ind} and $E_{x\ time}$ for crack analysis, has outcomes depicted in Table II. This Table shows that *CLAFCMC* outperforms all other variants, enabling effective identification of cracks in contaminated images. Although the KMC method executes more faster than the others, including *CLAFCMC*, but it underperforms for D_{Bl} (as compare with *CLAFCMC*). Therefore, based on the comprehensive findings in Table II and Fig. 5, *CLAFCMC* clearly delivers superior results compared to the alternatives.

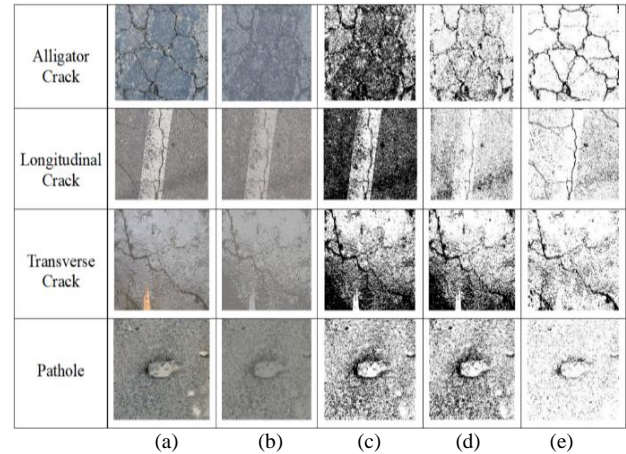


Figure 5: Crack detection (a) Original image, (b) KMC, (c) FCMC, (d) MHFCM, (e) *CLAFCMC*

4.3 Comparative analysis: proposed *CLAFCMC* vs. deep learning approaches

The proposed algorithm presents notable advantages when compared to deep learning methods like Convolutional Neural Networks (CNNs). The Proposed approach may operate effectively with smaller datasets and standard equipment's like CPU, in contrast to CNNs which require large datasets and powerful hardware [33]. Unlike CNNs, which demand a complex and lengthy training process, the *CLAFCMC* operates without any training, leading to much lower computational expenses. Furthermore, CNN interpretability is often limited [33]. Nonetheless, it is noteworthy that CNNs often do exceptionally well in handling intricate patterns, especially when trained on a variety of datasets, in terms of accuracy and adaptability. This makes them well-suited for tasks demanding high precision [33][34][35]. Consequently, *CLAFCMC* becomes a viable and economical option, especially valuable in situations where data or resources are limited.

5 Discussion

The experimental results clearly represent the effectiveness of the proposed method in precisely extracting road cracks from various types of images. Notably, the deficiencies found in KMC, FCMC, and MHFCM highlight the superiority of the proposed approach. KMC's reliance on preset clusters diminishes its accuracy when handling intricate data. FCMC's major limitation is its sensitivity to image noise, stemming from its disregard for pixel interconnections. MHFCM encounters processing difficulties, particularly with larger images, due to the complexities involved with FCMC and histogram equalization.

To overcome these limitations, the proposed method integrating \hat{I}_{pix}^{Cn} and A_{px}^e to enhance the crack segmentation accuracy. Unlike standard FCM's, it employs a $\hat{W}_{dow}^{(3 \times 3)}$ across the whole image ($k \times l$) for \hat{I}_{pix}^{Cn} , ensuring superior pixel classification and noise resilience.

The A_{px}^e refines crack detection by emphasizing intricate details and improving feature discernment. Additionally, the $i_{max,min}^d(g)$ examine to refine the ambiguity that arises in cluster assignments, resulting in more precise and reliable fracture identification. The *CLAFCMC* demonstrated exceptional performance in P_{ent} , D_{BI} , P_{ind} and $E_{x\ time}$, yielding values of 0.11, 0.50, 0.07, and 9.71 for non-paint-water strap images; 0.09, 0.52, 0.06, 10.12 for paint-water strap images. These results surpass all other methods tested.

A key highlight of *CLAFCMC* is its significantly reduced $E_{x\ time}$, which is a critical aspect of this study. Although *CLAFCMC* may be slightly slower than KMC in terms of $E_{x\ time}$, it surpasses all other algorithms in metrics like P_{ent} , D_{BI} , P_{ind} . The experimental results across various image types underscore the overall effectiveness and utility of the *CLAFCMC* algorithm.

6 Conclusion and future research

In this work, we introduce an innovative and novel approach based on FCMC clustering for road fracture identification. Despite the limited research on FCMC algorithm based on road crack detection, our method excels at identifying road cracks in images and effectively mitigates noise. The proposed method outperforming both the standard FCMC and its modifications. This is accomplished by applying a 3×3 window that spans the whole picture and classifying the pixels into edge or non-edge pixels prior to segmentation utilising a second order difference equation. This technique additionally permits edge pixel augmentation in every window, thereby enhancing the details of fissures to improve identification accuracy. Additionally, the intensity difference addressing the ambiguity that arises in cluster assignments when Euclidean distances are identical during segmentation, leading to more accurate and reliable fracture identification.

This leads to better performance since it improves clustering, precisely defines boundaries, and gets rid of crack blurring. In spite of images with low contrast, it effectively detects edges and fissures. Unlike many Fuzzy-C Means clustering variants, this method removes the need for determining crucial tuning parameters while consistently delivering better results, as confirmed by experimental findings. This algorithm reliably recognises fractures in novel and varied kinds of new images without the need of training. Extensive experimental outcomes illustrate efficacy of the *CLAFCMC* approach in terms of P_{ent} , D_{BI} , P_{ind} and $E_{x\ time}$. As an outcome, *CLAFCMC* is highly effective at identifying various types of road cracks. This timely detection helps the concerned person to apply the prompt maintenance process, preventing cracks from becoming more severe and thus indirectly leading to significant cost savings by avoiding extensive and critical repairs.

The upcoming project aims to outfit vehicles with an advanced online embedded system equipped with

high-quality cameras. This upgrade will facilitate the seamless capture and aggregation of real-time video feeds. Furthermore, a specialized technique will be designed to estimate the width & depth of road cracks using real-time data streams.

References

- [1] Diahao Ai, Guiyuan Jiang, Lam Siew Kei and Chengwu Li. Automatic Pixel-Level Pavement Crack Detection Using Information of Multi-Scale Neighborhoods. IEEE access, 6: 24452-24463, 2018. <https://doi.org/10.1109/ACCESS.2018.2829347>
- [2] Arun Mohan, Sumathi Poobal. Crack Detection using image processing: A critical review and analysis. Alexandria engineering journal, 57(2): 787-798, 2018. <https://doi.org/10.1016/j.aej.2017.01.020>
- [3] Munish Bhardwaj, Nafis Uddin Khan, Vikas Baghel. Fuzzy C-Means clustering based selective edge enhancement scheme for improved road crack detection. Engineering applications of Artificial Intelligence, 136, 1-14, 2024. <https://doi.org/10.1016/j.engappai.2024.108955>
- [4] Dan Wang, Zaijun Zhang, Jincheng Zhou, Benfei Zhang, and Mingjiang Li. Comparison and Analysis of Several Clustering Algorithms for Pavement Crack Segmentation Guided by Computational Intelligence. Hindawi computational intelligence and neuroscience, 2022(12):1-13, 2022. <https://doi.org/10.1155/2022/8965842>
- [5] Abdul Rahim Ahmad, Muhammad Khusairi Osman, Nor Aizam Muhammed Yusof. Image segmentation for pavement crack detection system. IEEE international conference on control system, computing and engineering, 153-157, 2020. <https://doi.org/10.1109/ICCSCCE50387.2020.9204935>
- [6] Munish Bhardwaj, Nafis Uddin Khan, Vikas Baghel, Santosh Kumar Vishwakarma, and Abul Bashar. Brain tumor image segmentation using K-means and Fuzzy C-Means clustering. Digital image enhancement and reconstruction Elsevier inc., 293-316, 2023. <https://doi.org/10.1016/B978-0-32-398370-9.00020-2>
- [7] James C. Bezdek, Robert Ehrlich, William Full. FCM: The Fuzzy C-Means clustering algorithm. Computers & geosciences, 10 (2-3): 191-203, 1984. [https://doi.org/10.1016/0098-3004\(84\)90020-7](https://doi.org/10.1016/0098-3004(84)90020-7)
- [8] Munish Bhardwaj, Nafis Uddin Khan, Vikas Baghel. Improved road crack detection using Histogram Equalization based Fuzzy-C Means technique. IEEE conference on PDGC, 547-551, 2023. <https://doi.org/10.1109/PDGC56933.2022.10053319>
- [9] Qingsheng Wang, Xiaopeng Wang, Chao Fang, Wnting Yang. Robust fuzzy c-means clustering algorithm with adaptive spatial & intensity

- constraint and membership linking for noise image segmentation. *Applied soft computing journal*, 92, 1-14, 2020.
<https://doi.org/10.1016/j.asoc.2020.106318>
- [10] Ming-Chuan Hung and Don-Lin Yang. An Efficient Fuzzy C-Means Clustering Algorithm. *IEEE International Conference on Data Mining*, 225-232, 2001.
<https://doi.org/10.1109/ICDM.2001.989523>
- [11] Munish Bhardwaj, Nafis Uddin Khan, Vikas Baghel. Road crack detection using pixel classification and intensity-based distinctive fuzzy C-means clustering. *The Visual Computer*, 41, 1689–1704 2025
<https://doi.org/10.1007/s00371-024-03470-8>
- [12] Youmeng Guan. An algorithm for data management of higher education based on Fuzzy Set Theory - association rule mining algorithm. *Informatica*, 45 (2021):157–164, 2023.
<https://doi.org/10.31449/inf.v47i9.5222>
- [13] M. Bhardwaj, N. U. Khan and V. Baghel. Road Crack Detection using Rooted Ratio-Dependent Scaling Factor and Pixel Difference based Fuzzy-C Means Clustering Technique. *IEEE Eighth International Conference on Parallel, Distributed and Grid Computing*, 212-217, 2024.
<https://doi.org/10.1109/PDGC64653.2024.10984164>
- [14] N. R. Pal and J. C. Bazdek. On cluster validity for the fuzzy c-means model. *IEEE Transactions on Fuzzy Systems*, 3(3), 370-379, 1995.
<https://doi.org/10.1109/91.413225>
- [15] Yohwan Noh, Donghyun Koo, Yong-Min Kang, Dong Gyu Park, DoHoon Lee, Panop Khumsap. Automatic crack detection on concrete images using segmentation via Fuzzy C-means clustering. *IEEE international conference on applied system innovation*, 877-880, 2017.
<https://doi.org/10.1109/ICASI.2017.7988574>
- [16] A. Cubero Fernandez, Fco. J. Rodriguez Lozano, Rafael Villatoro, Joaquin Olivares and Jose M. Palomares. Palomares. Efficient pavement crack detection and classification. *EURASIP journal on image and video processing*, 39:1-11, 2017.
<https://doi.org/10.1186/s13640-017-0187-0>
- [17] Yashon O. Oumaa, M. Hahn. Pothole detection on asphalt pavements from 2D-colour pothole images using Fuzzy c-means clustering and morphological reconstruction. *Automation and construction*, 83: 196-211, 2017.
<https://doi.org/10.1016/j.autcon.2017.08.017>
- [18] Yong Shi, Limeng Cui, Zhiquan Qi, Fan Meng, and Zhensong Chen. Automatic road crack detection using Random Structured Forests. *IEEE transactions on intelligent transportations systems*, 17(12):3434-3445, 2016.
<https://doi.org/10.1109/TITS.2016.2552248>
- [19] Weixing Wang, Lei Li, Ya Han. Crack detection in shadowed images on gray level deviations in a moving window and distance deviations between connected components. *Construction and building material elsevier*, 271: 1-12, 2021.
<https://doi.org/10.1016/j.conbuildmat.2020.121885>
- [20] C. Gou, B. Peng, T. Li and Z. Gao. Pavement Crack Detection Based on the Improved Faster-RCNN.II; *IEEE 14th International Conference on Intelligent Systems and Knowledge Engineering (ISKE)*, 962-967, 2019.
<https://doi.org/10.1109/ISKE47853.2019.9170456>
- [21] Xiaoran Feng, Liyang Xiao, Wei Li, Lili Pei, Zhaoyun Sun, Zhidan Ma, Hao Shen, and Huyan Ju. Pavement Crack Detection and Segmentation Method Based on Improved Deep Learning Fusion Model. *Hindawi Mathematical Problems in Engineering*, 2020(1), 1-22, 2020.
<https://doi.org/10.1155/2020/8515213>
- [22] Jie Luo, Huazhi Lin, Xiaoxu Wei and Yongsheng Wang. Adaptive Canny and Semantic segmentation Networks based on Feature Fusion for road crack detection. *IEEE access*, 11:51740- 51753, 2023.
<https://doi.org/10.1109/ACCESS.2023.3279888>
- [23] Chengjia Han, Tao Ma, Ju Huyan, Xiaoming Huang, and Yanning Zhang. Crack W-Net: A Novel Pavement Crack Image Segmentation Convolutional Neural Network. *IEEE Transactions on Intelligent Transportations Systems*, 23 (11), 22135- 22144, 2021. <https://doi.org/10.1109/TITS.2021.3095507>
- [24] Li Fan and Jiancheng Zou. A Novel Road Crack Detection Technology Based on Deep Dictionary Learning and Encoding Networks. *MDPI applied sciences*, 13(22), 1-20, 2023.
<https://doi.org/10.3390/app132212299>
- [25] Weidong Song, Guohui Jia, Di Jia and Hong Zhu. Automatic Pavement Crack Detection and Classification Using Multiscale Feature Attention Network. *IEEE Access*, 7, 171001- 171012, 2019.
<https://doi.org/10.1109/ACCESS.2019.2956191>
- [26] Jong-Hyun Kim and Jung Lee. Efficient Dataset Collection for Concrete Crack Detection with Spatial-Adaptive Data Augmentation. *IEEE Access*, 11, 121902-121913, 2023.
<https://doi.org/10.1109/ACCESS.2023.3328243>
- [27] Rafael C. Gonzalez, Richrad E Woods. *Digital image processing*. Pearson Hall, 2002.
- [28] Balazs Balasko, Janos Abonyi and Balazs Feil. *Fuzzy Clustering and Data Analysis Toolbox for Use with Matlab*. 1-74, 2014.
<https://www.researchgate.net/publication/263697045>
- [29] Leonardo Enzo Brito da Silva, Niklas M. Melton, Donald C. Wunsch II. Incremental Cluster Validity Indices for Hard Partitions: Extensions and Comparative Study, *arXiv*, 1-31, 2019.
<https://doi.org/10.48550/arXiv.1902.06711>
- [30] Mohamed Abdellatif, Harriet Peel, Anthony G. Cohn, Raul Fuentes. Combining block-based and pixel-based approaches to improve crack detection and localization. *Automation in Construction*. 122, 1-14, 2021.
<https://doi.org/10.1016/j.autcon.2020.103492>

- [31] Florent Forest, Hugo Porta, Devis Tuia, Olga Fink. From classification to segmentation with explainable AI: A study on crack detection and growth monitoring. *Automation in Construction*, 165, 1-16 2024.
<https://doi.org/10.1016/j.autcon.2024.105497>
- [32] Yixiong Jing, Jia-Xing Zhong, Brian Sheil, Sinan Acikgoz. Anomaly detection of cracks in synthetic masonry arch bridge point clouds using fast point feature histograms and PatchCore. *Automation in Construction*, 168, 1-13, 2024.
<https://doi.org/10.1016/j.autcon.2024.105766>
- [33] Yujun Wang. Deep Learning models in computer data mining for intrusion detection. *Informatica*, 47:555–568, 2023.
<https://doi.org/10.31449/inf.v47i4.4942>
- [34] Munish Bhardwaj, Nafis Uddin khan, Vikas Baghel, “A Novel Fuzzy C-Means Clustering Framework for Accurate Road Crack Detection: Incorporating Pixel Augmentation and Intensity Difference Features”, *Informatica* 49:27–40, 2025.
<https://doi.org/10.31449/inf.v49i15.7082>
- [35] Ming Zhu, Yongning He, Qingyu He. A review of researches on Deep Learning in Remote Sensing application. *International journal of geosciences*, 10(1):1-11, 2019.
<https://doi.org/10.4236/ijg.2019.101001>